

A New Algorithm For Solving Thermal Newtonian Flow In Axisymmetric Straight Channel

Anas Al-Haboobi^{1,2}, Alaa H. Al-Muslimawi^{2, *}

1. Department of Mathematics, College of Science, University of Basrah, Basra, Iraq.

2. Department of Postgraduate Studies, University of Kufa, Kufa, Iraq.

*Corresponding author E-mail: alaa.abdullah@uobasrah.edu.iq

Doi:10.29072/basjs.20230301

<u>ARTICLE INFO</u>	<u>ABSTRACT</u>
<p>Keywords</p> <p>Finite element method</p> <p>Taylor-Galerkin /Pressure-Correction method</p> <p>thermal flow</p> <p>incompressible flow</p> <p>Newtonian flow</p>	<p>In this study, three main problems in fluid flow have been discussed. First, the derivation of the energy equation is conducted within cylindrical coordinates, which has not been addressed by the researchers before. Secondly, we develop a new algorithm for solving the governing equations that describe incompressible Newtonian flows under thermal condition. This algorithm is constructed based on the so-called Taylor-Galerkin/Pressure-Correction finite element method with the help of the two-step Lax-Wendroff scheme. Finally, we study the effect of non-dimensional numbers, such as the Reynolds number (Re) and the Prandtl number (Pr), on the velocity, pressure, and temperature. The results show that the developed method is consistent with established physical phenomena and other studies.</p>

Received 11 Aug 2023; Received in revised form 12 Oct 2023; Accepted 30 Nov 2023, Published 31 Dec 2023



1. Introduction

Non-isothermal flow refers to the flow of fluid at temperatures that are not uniform. As the temperature of the fluid changes, its material properties, including density, viscosity, and thermal conductivity, can also change. These changes can have a significant impact on the flow field. Moreover, because the fluid is also responsible for transporting heat, any changes in the flow field can affect the temperature field, resulting in a two-way coupling between fluid flow and heat transfer. This phenomenon is commonly observed in various applications, including heat exchangers, chemical reactors, atmospheric flows, and cooling processes. Understanding this two-way coupling is essential to comprehensively analyze and optimize these systems. In recent years, heat transfer and its impact on fluid flow have been extensively studied due to its fundamental importance in various branches of engineering [1-3]. The application of engineering design procedures to non-isothermal laminar flow of viscous Newtonian incompressible fluids forced through channels or tubes at a temperature different from that of the fluid is challenging. To tackle these problems, the Taylor-Galerkin/Pressure-Correction (TG/PC) finite element method is a suitable approach due to its high accuracy and efficiency. This method was initially proposed by Townsend and Webster [4] to handle isothermal viscous incompressible flows of both Newtonian and non-Newtonian fluids. It has been widely adopted in the literature for isothermal flows, as seen in the works of Ngamaramvaranggul and Webster [5], Ngamaramvaranggul and Thongjub [6], Al-Haboobi et al. [7], Al-Muslimawi [8], Abro et al. [9], among others. The key distinction between this method and earlier ones is that it separates the velocity and pressure variables. This separation concept is based on Chorin's work [10]. In the past, the fractional step method, favored by Gresho et al. [11] and Donea et al. [12], or the velocity correction approach, used by Kawahara and Ohmiya [13], were utilized to solve the governing equations of flow. Notably, the significant difference between these methods is that, for the former, the separation of velocity and pressure is performed after the differential equations are discretized using the GFEM, while for the latter, it occurs at the differential equation stage. Through our work, we aim to determine the effect of various factors, such as Reynolds number and Prandtl number, on steady-state flow by solving the presented equations using the TG/PC method. The main objective of this study is to derive the energy equation within cylindrical polar coordinates and develop a new code to simulate incompressible Newtonian fluids under non-isothermal conditions. A novel and highly accurate method for solving the governing differential equations is proposed, which is a combination of



new fractional steps for energy within the Taylor-Galerkin/Pressure-Correction (TG/PC) method, called the Developed Taylor-Galerkin/Pressure-Correction (DTG/PC) method. This is the first time that such a technique has been applied to this type of problem. The proposed method includes applying the two steps Lax-Wendroff method to the energy equation to obtain two new fractional steps for temperature, which merge with the algorithm according to the required priority. The study also investigates the temporal convergence rate of the system solution, which is assumed to be steady state, incompressible, axisymmetric, and laminar, a topic not previously addressed by researchers. Additionally, the study evaluates three types of meshes and selects the most appropriate ones for studying the results. Furthermore, the study examines the direct effects of important parameters on the motion and temperature of the fluid, such as the Reynolds number (Re) and Prandtl number (Pr) for each of velocity and temperature. The method's convergence is also guaranteed. The organization of this paper is as follows: section 2 present the mathematical modeling of Newtonian non-isothermal flow motion with show how to convert the modeling in a non-dimensional form. In section 3 we introduce the developed Taylor-Galerkin/Pressure-Correction algorithm (DTG/PC) by highlighting the new steps added about temperature and exhibition of all the necessary details of the finite element method (weak form and matrix formulation). The problem Specification and the related numerical findings are presented in Section 4 and 5, respectively.

2. Mathematical Modeling

The system of equations for incompressible Newtonian non-isothermal flow in cylindrical coordinates will be introduced as follows: [14-16]

Conservation of mass

$$\nabla \cdot \mathbf{u} = 0 . \quad (1)$$

In component form

$$\frac{1}{r} \frac{\partial(r u_r)}{\partial r} + \frac{1}{r} \frac{\partial(u_\theta)}{\partial \theta} + \frac{\partial(u_z)}{\partial z} = 0 . \quad (2)$$

Conservation of momentum

$$\rho \frac{\partial \mathbf{u}}{\partial t} = \mu \nabla^2 \mathbf{u} - \rho(\mathbf{u} \cdot \nabla) \mathbf{u} - \nabla p . \quad (3)$$



In component form

r-direction

$$\frac{\partial u_r}{\partial t} + u_r \frac{\partial u_r}{\partial r} + \frac{u_\theta}{r} \frac{\partial u_r}{\partial \theta} + u_z \frac{\partial u_r}{\partial z} - \frac{u_\theta^2}{r} = -\frac{1}{\rho} \frac{\partial p}{\partial r} + \frac{\mu}{\rho} \left[\frac{1}{r} \frac{\partial}{\partial r} \left(r \frac{\partial u_r}{\partial r} \right) + \frac{1}{r^2} \frac{\partial^2 u_r}{\partial \theta^2} + \frac{\partial^2 u_r}{\partial z^2} - \frac{2}{r^2} \frac{\partial u_\theta}{\partial \theta} - \frac{u_r}{r^2} \right]. \quad (4)$$

θ -direction

$$\frac{\partial u_\theta}{\partial t} + u_r \frac{\partial u_\theta}{\partial r} + \frac{u_\theta}{r} \frac{\partial u_\theta}{\partial \theta} + u_z \frac{\partial u_\theta}{\partial z} + \frac{u_r u_\theta}{r} = -\frac{1}{\rho} \frac{1}{r} \frac{\partial p}{\partial \theta} + \frac{\mu}{\rho} \left[\frac{1}{r} \frac{\partial}{\partial r} \left(r \frac{\partial u_\theta}{\partial r} \right) + \frac{1}{r^2} \frac{\partial^2 u_\theta}{\partial \theta^2} + \frac{\partial^2 u_\theta}{\partial z^2} + \frac{2}{r^2} \frac{\partial u_r}{\partial \theta} - \frac{u_\theta}{r^2} \right]. \quad (5)$$

z-direction

$$\frac{\partial u_z}{\partial t} + u_r \frac{\partial u_z}{\partial r} + \frac{u_\theta}{r} \frac{\partial u_z}{\partial \theta} + u_z \frac{\partial u_z}{\partial z} = -\frac{1}{\rho} \frac{\partial p}{\partial z} + \frac{\mu}{\rho} \left[\frac{1}{r} \frac{\partial}{\partial r} \left(r \frac{\partial u_z}{\partial r} \right) + \frac{1}{r^2} \frac{\partial^2 u_z}{\partial \theta^2} + \frac{\partial^2 u_z}{\partial z^2} \right]. \quad (6)$$

Now, we have to introduce the derivation of the energy equation in the cylindrical coordinate.

The energy balance is defined as

$$\underbrace{\text{Energy Stored}}_{E_{st}} = \underbrace{\text{Energy Entering}}_{E_{in}} - \underbrace{\text{Energy Leaving}}_{E_{out}} + \underbrace{\text{Energy Generation}}_{E_{gen}}. \quad (7)$$

Consider the rate at which thermal energy is being stored is proportional to the heat capacity as:

$$\begin{aligned} E_{st} &= MC_p \frac{DT}{Dt}, \\ &= \rho V C_p \frac{DT}{Dt}, \\ &= \rho (dr r d\theta dz) C_p \frac{DT}{Dt}, \\ &= \rho C_p \frac{DT}{Dt} dr r d\theta dz. \end{aligned} \quad (8)$$

The energy entering E_{in} is defined as

$$E_{in} = q_r + q_\theta + q_z, \quad (9)$$



thus, the energy Leaving E_{out} is defined as:

$$E_{out} = q_r + dr + q_\theta + d\theta + q_z + dz , \quad (10)$$

by using Fourier's law of heat conduction (see [17]) the equations (9) and (10) will be re-written as:

$$E_{in} = -k \frac{\partial T}{\partial r} r d\theta dz - k \frac{\partial T}{r \partial \theta} dr dz + -k \frac{\partial T}{\partial z} dr r d\theta, \quad (11)$$

$$E_{out} = -k \frac{\partial T}{\partial r} r d\theta dz - \frac{\partial}{\partial r} \left(k r \frac{\partial T}{\partial r} \right) dr d\theta dz - k \frac{\partial T}{r \partial \theta} dr dz - \frac{\partial}{\partial \theta} \left(k \frac{\partial T}{r \partial \theta} \right) dr d\theta dz, \quad (12)$$

$$-k \frac{\partial T}{\partial z} dr r d\theta - \frac{\partial}{\partial z} \left(k \frac{\partial T}{\partial z} \right) dr r d\theta dz,$$

lastly, we need to consider the rate of thermal energy generation as:

$$E_{gen} = \Phi \times \text{Volume} , \quad (13)$$

$$= \Phi dr r d\theta dz.$$

Now, By substituting equations (8), (11), (12) and (13) in (7) we get

$$\rho C_p \frac{DT}{Dt} dr r d\theta dz = \frac{\partial}{\partial r} \left(k r \frac{\partial T}{\partial r} \right) dr d\theta dz + \frac{\partial}{\partial \theta} \left(k \frac{\partial T}{r \partial \theta} \right) dr d\theta dz + \frac{\partial}{\partial z} \left(k \frac{\partial T}{\partial z} \right) dr r d\theta dz + \Phi dr r d\theta dz. \quad (14)$$

Then, dividing equation (14) by ($dr r d\theta dz$), we get the energy equation in the form: of conservation of energy

$$\rho C_p \left[\frac{\partial T}{\partial t} + (u \cdot \nabla) T \right] = k \nabla^2 T + \Phi. \quad (15)$$

In component form

$$\rho C_p \left[\frac{\partial T}{\partial t} + u_r \frac{\partial T}{\partial r} + \frac{u_\theta}{r} \frac{\partial T}{\partial \theta} + u_z \frac{\partial T}{\partial z} \right] = k \left[\frac{1}{r} \frac{\partial}{\partial r} \left(r \frac{\partial T}{\partial r} \right) + \frac{1}{r^2} \frac{\partial^2 T}{\partial \theta^2} + \frac{\partial^2 T}{\partial z^2} \right] + \Phi. \quad (16)$$

Where, u , ρ , p and μ are the velocity, density, pressure and viscosity of the fluid, respectively. Moreover, T is the fluid temperature, C_p is the thermal heat capacity at constant pressure, k is the thermal conductivity, and Φ is a dissipation function dependent on shear rate.

Now, we have to define the non-dimensionalization of the conservation (of mass, momentum and energy) equations as follows [18,19]

$$t^* = \frac{t}{L/U_\infty}, u^* = \frac{u}{U_\infty}, p^* = \frac{p - p_\infty}{\rho U_\infty^2}, T^* = \frac{T - T_\infty}{\Delta T}, \nabla = \frac{1}{L} \nabla^*,$$

where, U_∞ is the characteristic velocity, p_∞ is the characteristic pressure, T_∞ is the characteristic temperature,



L is the characteristic length, and ΔT is a known reference temperature difference in the flow field such as the one between a constant wall temperature (if it exists) and T_∞ . Now by using the definition of non-dimensionalization in the governing equations, the equations (1) - (6) and (15), (16) can be converted into the following ones and the superscript * has been skipped for convenience:

Conservation of mass

$$\nabla \cdot \mathbf{u} = 0. \quad (17)$$

In component form

$$\frac{1}{r} \frac{\partial(ru_r)}{\partial r} + \frac{1}{r} \frac{\partial(u_\theta)}{\partial \theta} + \frac{\partial(u_z)}{\partial z} = 0. \quad (18)$$

Conservation of momentum

$$Re \frac{\partial \mathbf{u}}{\partial t} = \mu \nabla^2 \mathbf{u} - \rho(\mathbf{u} \cdot \nabla) \mathbf{u} - \nabla p. \quad (19)$$

In component form

r-direction

$$\begin{aligned} \frac{\partial u_r}{\partial t} + u_r \frac{\partial u_r}{\partial r} + \frac{u_\theta}{r} \frac{\partial u_r}{\partial \theta} + u_z \frac{\partial u_r}{\partial z} - \frac{u_\theta^2}{r} = -\frac{1}{Re} \frac{\partial p}{\partial r} \\ + \frac{\mu}{Re} \left[\frac{1}{r} \frac{\partial}{\partial r} \left(r \frac{\partial u_r}{\partial r} \right) + \frac{1}{r^2} \frac{\partial^2 u_r}{\partial \theta^2} + \frac{\partial^2 u_r}{\partial z^2} - \frac{2}{r^2} \frac{\partial u_\theta}{\partial \theta} - \frac{u_r}{r^2} \right]. \end{aligned} \quad (20)$$

θ -direction

$$\begin{aligned} \frac{\partial u_\theta}{\partial t} + u_r \frac{\partial u_\theta}{\partial r} + \frac{u_\theta}{r} \frac{\partial u_\theta}{\partial \theta} + u_z \frac{\partial u_\theta}{\partial z} + \frac{u_r u_\theta}{r} = -\frac{1}{Re} \frac{1}{r} \frac{\partial p}{\partial \theta} \\ + \frac{\mu}{Re} \left[\frac{1}{r} \frac{\partial}{\partial r} \left(r \frac{\partial u_\theta}{\partial r} \right) + \frac{1}{r^2} \frac{\partial^2 u_\theta}{\partial \theta^2} + \frac{\partial^2 u_\theta}{\partial z^2} + \frac{2}{r^2} \frac{\partial u_r}{\partial \theta} - \frac{u_\theta}{r^2} \right]. \end{aligned} \quad (21)$$

z-direction

$$\begin{aligned} \frac{\partial u_z}{\partial t} + u_r \frac{\partial u_z}{\partial r} + \frac{u_\theta}{r} \frac{\partial u_z}{\partial \theta} + u_z \frac{\partial u_z}{\partial z} = -\frac{1}{Re} \frac{\partial p}{\partial z} \\ + \frac{\mu}{Re} \left[\frac{1}{r} \frac{\partial}{\partial r} \left(r \frac{\partial u_z}{\partial r} \right) + \frac{1}{r^2} \frac{\partial^2 u_z}{\partial \theta^2} + \frac{\partial^2 u_z}{\partial z^2} \right]. \end{aligned} \quad (22)$$



$$RePr \left[\frac{\partial T}{\partial t} + (u \cdot \nabla)T \right] = \nabla^2 T + \frac{Ec}{Re} \Phi. \quad (23)$$

In component form

$$RePr \left[\frac{\partial T}{\partial t} + u_r \frac{\partial T}{\partial r} + \frac{u_\theta}{r} \frac{\partial T}{\partial \theta} + u_z \frac{\partial T}{\partial z} \right] = \left[\frac{1}{r} \frac{\partial}{\partial r} \left(r \frac{\partial T}{\partial r} \right) + \frac{1}{r^2} \frac{\partial^2 T}{\partial \theta^2} + \frac{\partial^2 T}{\partial z^2} \right] + \frac{Ec}{Re} \Phi. \quad (24)$$

In these equations there are three non-dimensional numbers, the Reynolds number defined by

$$Re = \frac{\rho U_\infty L}{\mu},$$

the Prandtl number is defined by

$$Pr = \frac{\mu}{k/Cp},$$

and the Eckert number is defined by

$$Ec = \frac{U_\infty^2}{Cp\Delta t}.$$

3. Numerical Method

In this section, we discuss the development of the Taylor-Galerkin/Pressure-Correction method (TG/PC) for solving the system equations of incompressible Newtonian fluids under non-isothermal conditions. The TG/PC method is a fractional step method that semi-discretizes the equations first in the temporal domain using Taylor series expansions in time, followed by a pressure-correction procedure. This numerical technique was introduced by Townsend and Webster to solve incompressible isothermal flow [4].

Now, by applying the Lax-Wendroff scheme [20] to the equation (19) and (23), we have

Conservation of momentum equation became:

$$\begin{aligned} \text{step 1: } \quad u^{n+1/2} &= u^n + \frac{\Delta t}{2Re} (L(u^n) - \nabla p^n), \\ \text{step 2: } \quad u^{n+1} &= u^n + \frac{\Delta t}{Re} (L(u^{n+1/2}) - \nabla p^{n+1/2}), \end{aligned} \quad (25)$$



where,

$$L(u) = \mu \nabla^2 u - \text{Re}(u \cdot \nabla)u.$$

Likewise, the conservation of energy equation became:

$$\begin{aligned} \text{step 1: } T^{n+1/2} &= T^n + \frac{\Delta t}{2\text{RePr}} G(u^n, T^n), \\ \text{step 2: } T^{n+1} &= T^n + \frac{\Delta t}{\text{RePr}} G(u^{n+1/2}, T^{n+1/2}), \end{aligned} \quad (26)$$

where,

$$G(u, T) = \nabla^2 T + \frac{Ec}{Re} \Phi - \text{RePr}(u \cdot \nabla)T.$$

We shall approximate the pressure $p^{n+1/2}$ in equation (25) (step 2) by

$$p^{n+1/2} = \varrho p^{n+1} + (1 - \varrho)p^n, \quad (27)$$

now, by substituting equation (27) in equation (25) (step 2), we get

$$u^{n+1} = u^n + \frac{\Delta t}{Re} (L(u^{n+1/2}) - \varrho \nabla p^{n+1} - (1 - \varrho) \nabla p^n). \quad (28)$$

Assume an intermediate velocity u^* such that

$$u^* = u^n + \frac{\Delta t}{Re} (L(u^{n+1/2}) - \nabla p^n). \quad (29)$$

Subtracting equation (29) from equation (28), we get

$$u^{n+1} = u^* - \frac{\varrho \Delta t}{Re} \nabla q^{n+1}. \quad (30)$$

where $q^{n+1} = p^{n+1} - p^n$.

Taking the divergence of equation (30) with $\nabla \cdot u^{n+1} = 0$, then we have

$$\nabla^2 q^{n+1} = \frac{Re}{\varrho \Delta t} \nabla \cdot u^*. \quad (31)$$

Thus, from equations (25a), (26), (29), (30) and (31) we can solve the system of equations in the following order

$$\text{stage 1: } u^{n+1/2} = u^n + \frac{\Delta t}{2\text{Re}} (L(u^n) - \nabla p^n), \quad (32)$$

$$\text{stage 2: } T^{n+1/2} = T^n + \frac{\Delta t}{2\text{RePr}} G(u^n, T^n), \quad (33)$$

$$\text{stage 3: } u^* = u^n + \frac{\Delta t}{Re} (L(u^{n+1/2}) - \nabla p^n), \quad (34)$$



$$\text{stage 4: } T^{n+1} = T^n + \frac{\Delta t}{\text{RePr}} G(u^{n+1/2}, T^{n+1/2}), \tag{35}$$

$$\text{stage 5: } \nabla^2 q^{n+1} = \frac{\text{Re}}{\rho \Delta t} \nabla \cdot u^*, \tag{36}$$

$$\text{stage 6: } u^{n+1} = u^* - \frac{\rho \Delta t}{\text{Re}} \nabla q^{n+1}. \tag{37}$$

These stages can be re-written in the matrix-vector form as

$$\text{stage 1: } \frac{2\text{Re}}{\Delta t} M \Delta U^{n+1/2} = L^T P^n - \mu D U^n - \text{Re } N(U^n) U^n + B, \tag{38}$$

$$\text{stage 2: } \frac{2\text{RePr}}{\Delta t} M \Delta T^{n+1/2} = -\text{Re Pr } (N(T^n) U^n) - D T^n + B + \Phi, \tag{39}$$

$$\text{stage 3: } \frac{\text{Re}}{\Delta t} M \Delta U^* = L^T P^n - \mu D U^{n+1/2} - \text{Re } N(U^{n+1/2}) U^{n+1/2} + B, \tag{40}$$

$$\text{stage 4: } \frac{\text{RePr}}{\Delta t} M \Delta T^{n+1} = -\text{Re Pr } (N(T^{n+1/2}) U^{n+1/2}) - D T^{n+1/2} + B + \Phi, \tag{41}$$

$$\text{stage 5: } K Q^{n+1} = -\frac{\text{Re}}{\rho \Delta t} L U^*, \tag{42}$$

$$\text{stage 6: } \frac{\text{Re}}{\Delta t} M \Delta U^{n+1} = \rho L^T Q^{n+1}, \tag{43}$$

where, $\Delta U^{n+1/2} = U^{n+1/2} - U^n$, $\Delta U^{n+1} = U^{n+1} - U^*$, $\Delta T^{n+1/2} = T^{n+1/2} - T^n$, $\Delta T^{n+1} = T^{n+1} - T^n$ and $\Delta U^* = U^* - U^n$. U is the velocity vector, T is the temperature vector and P is the pressure vector. Pressure difference vector defined as $Q^{n+1} = P^{n+1} - P^n$

The notation and structure of matrix been described below:

$$M_{ij} = [\phi_i, \phi_j] = \int_{\Omega} \phi_i \cdot \phi_j d\Omega, L_{ij} = (\psi_i, \nabla \cdot \phi_j) = \int_{\Omega} \psi_i \nabla \cdot \phi_j d\Omega$$

$$D_{ij} = [\nabla \phi_i, \nabla \phi_j] = \int_{\Omega} \nabla \phi_i \cdot \nabla \phi_j d\Omega, K_{ij} = [\nabla \psi_i, \nabla \psi_j] = \int_{\Omega} \nabla \psi_i \cdot \nabla \psi_j d\Omega$$

$$N(U)_{ij} = [\phi_i, u \cdot \nabla \phi_j] = \int_{\Omega} \left(\sum_l \phi_i \phi_j U^l \cdot \nabla \right) \phi_j d\Omega$$

$$N(T)_{ij} = [\phi_i, T \cdot \nabla \phi_j] = \int_{\Omega} \left(\sum_l \phi_i \phi_j T^l \cdot \nabla \right) \phi_j d\Omega,$$

$$B_i = [\phi_i, g]_{\Gamma} = \int_{\Gamma} g \cdot \phi_i d\Gamma,$$

where, B is a natural boundary condition vector and g is a given function.



4. Problem Specification and boundary conditions

In this section we study Poiseuille (Ps) flow through a two-dimensional axisymmetric rectangular channel with length $L = 2$ and height $H = 1$ taken under non-isothermal condition flow in cylindrical coordinates. For this context, three different triangular finite element meshes are implemented, coarse, normal and fine as shown in Figure 1. The finite element meshes characteristics are introduced in Table 1.

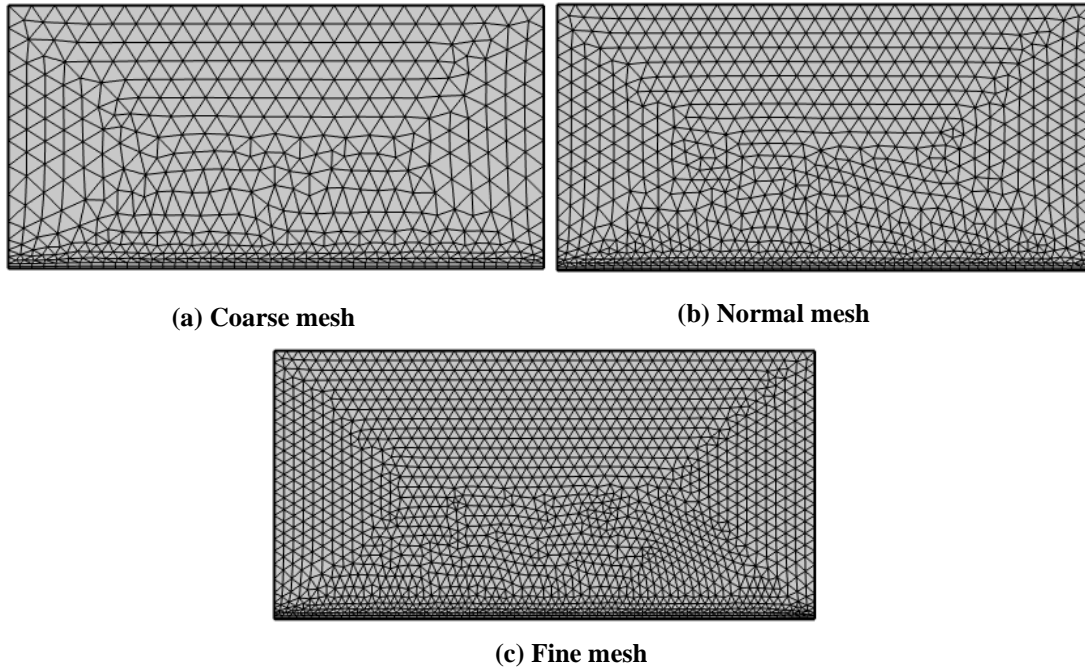


Figure 1: Different configuration of the meshes (a) Coarse mesh (b) Normal mesh (c) Fine mesh.

Table 1: Type of the achieved meshes.

Mesh	Total Elements	Number of vertices	Degrees of freedom
Coarse	1040	615	2460
Normal	1679	960	3840
Fine	3251	1783	7132

The boundary conditions for velocity and temperature in the problem under study will be set as follows:

1. At the inlet, we specified a Poiseuille flow with a corresponding analytical expression for fully-developed axial velocity given by $u_z = u_{max}(1 - r^2)$. where u_{max} is the maximum axial velocity, r is the radial coordinate, and u_z is the axial velocity component. This flow is commonly known as a Poiseuille flow and is characterized by a parabolic velocity profile. More details on the analytical expressions for this flow can be found in [21]. Additionally, we applied a specific temperature at the inlet.
2. On the top wall of the channel, no-slip BCs applied for velocity and pressure. We applied heat flux for temperature.
3. Along the outlet of the channel, we impose zero radial velocity and temperature, as well as zero pressure.

5. Numerical Results and Analysis

The problem is solved under consideration by using the developed Taylor-Galerkin/ Pressure-Correction method (DTG/PC). This is the first time we are solving the system of Navier Stokes equations under thermal conditions using this technique. We study the variation that occurs in fluid velocity and temperature to the three different meshes considered in the previous section. Also the effect of Reynolds number (Re) and Prandtl number (Pr) on velocity, pressure, and temperature is presented. The convergence rate for all components of solution is examined as well.

Mesh Convergence: We intend to show the velocity (u) profile at the outlet of the channel and the temperature (T) profile on the axisymmetric of the channel for different mesh configurations. As shown in Figure 2, improving the density of the meshes results in improved accuracy, and the problem becomes mesh-independent with a fine mesh. For this reason, the fine mesh for further computations is used.



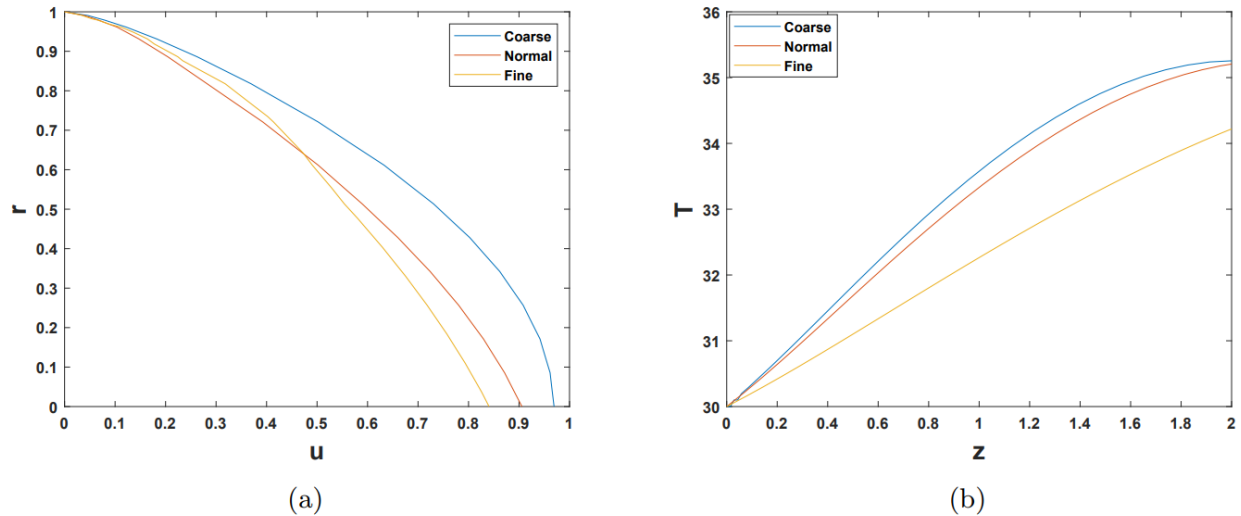


Figure 2: Plot of mesh Convergence for (a) Velocity and (b) Temperature.

Re-Variation: The importance of the Reynolds number (Re) is that it determines the quality of the liquid and its transition from the state of laminar flow to the turbulent flow, where if the Reynolds number exceeds the limit of 2300, the liquid turns into a turbulent flow (see [21]). Here, we investigate the effect of (Re) on each of the velocity (u), pressure (p) and temperature (T) at $\{Re = 1, 5, 10, 20\}$ with fixed Prandtl number (Pr) and viscosity (μ) $\{Pr = \mu = 1\}$. Figure 3 shows that when (Re) increases then both velocity and pressure value will be increase too, the reason is due that when (Re) increases, the flow rate increases, and therefore both the velocity and pressure of the flow increase (see [22]). Figure 4 displays the effect of (Re) on the velocity field in 2 Dimension (2D) and 3 Dimension (3D). In contrast, the effect of (Re) with fixed viscosity ($\mu = 1$) and Prandtl number ($Pr = 1$) with temperature is the reverse effect as shown in the Figures 5 and 6 with 2D and 3D. This is based on the fact that when (Re) increases, the flow of the fluid increases, which, leads to an increase in its velocity and, consequently, the difficulty of penetration of temperature into the fluid [23]. The relation between velocity and temperature is plotted in Figure 7.



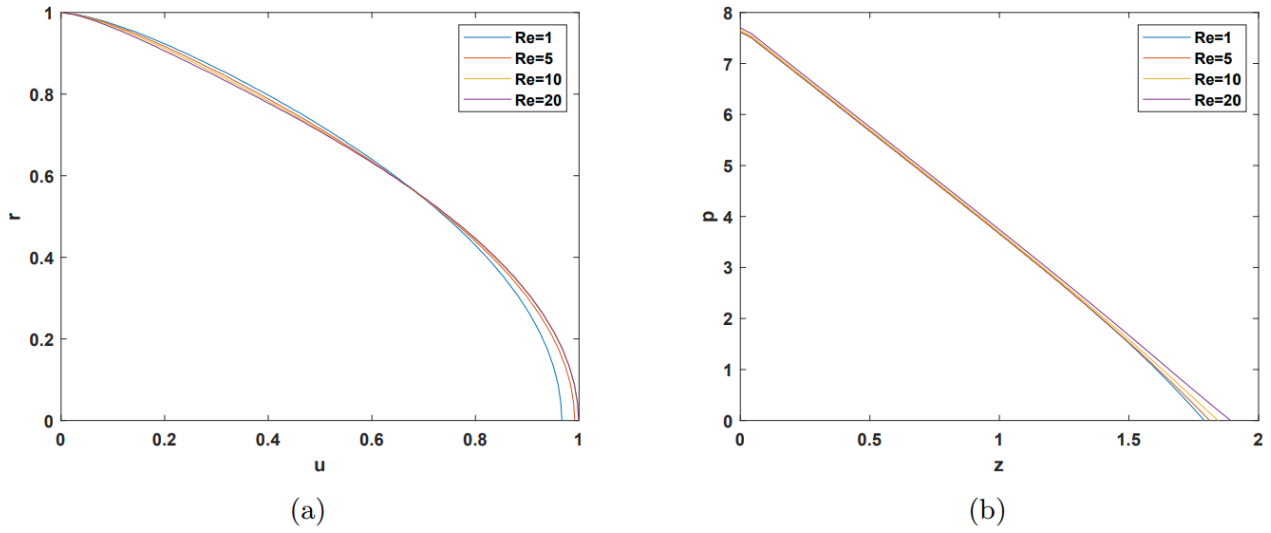


Figure 3: Effect Re on (a)Velocity and (b)Pressure.

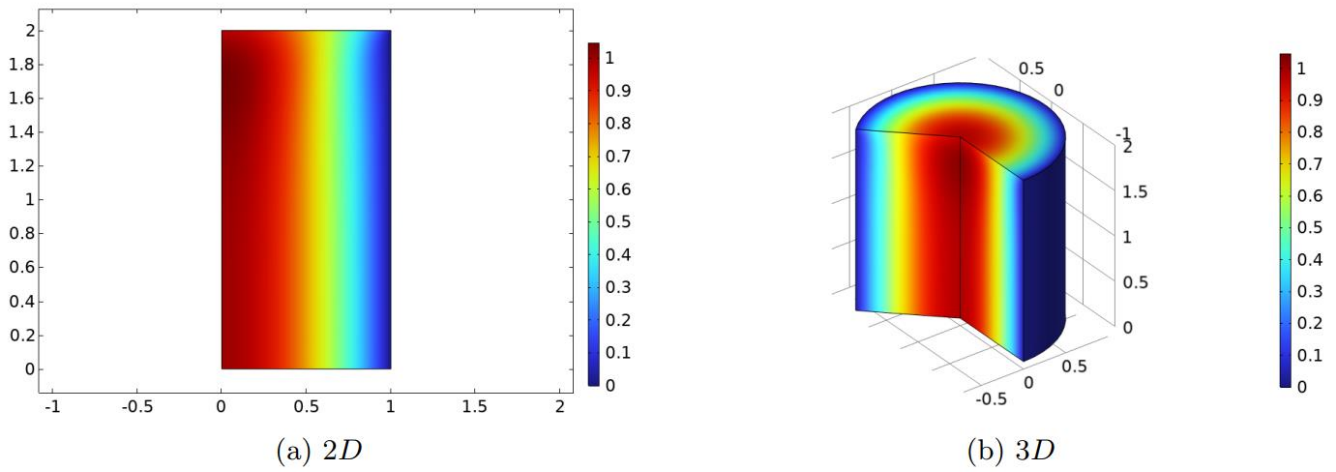


Figure 4: Effect Re on 2D and 3D Velocity field.



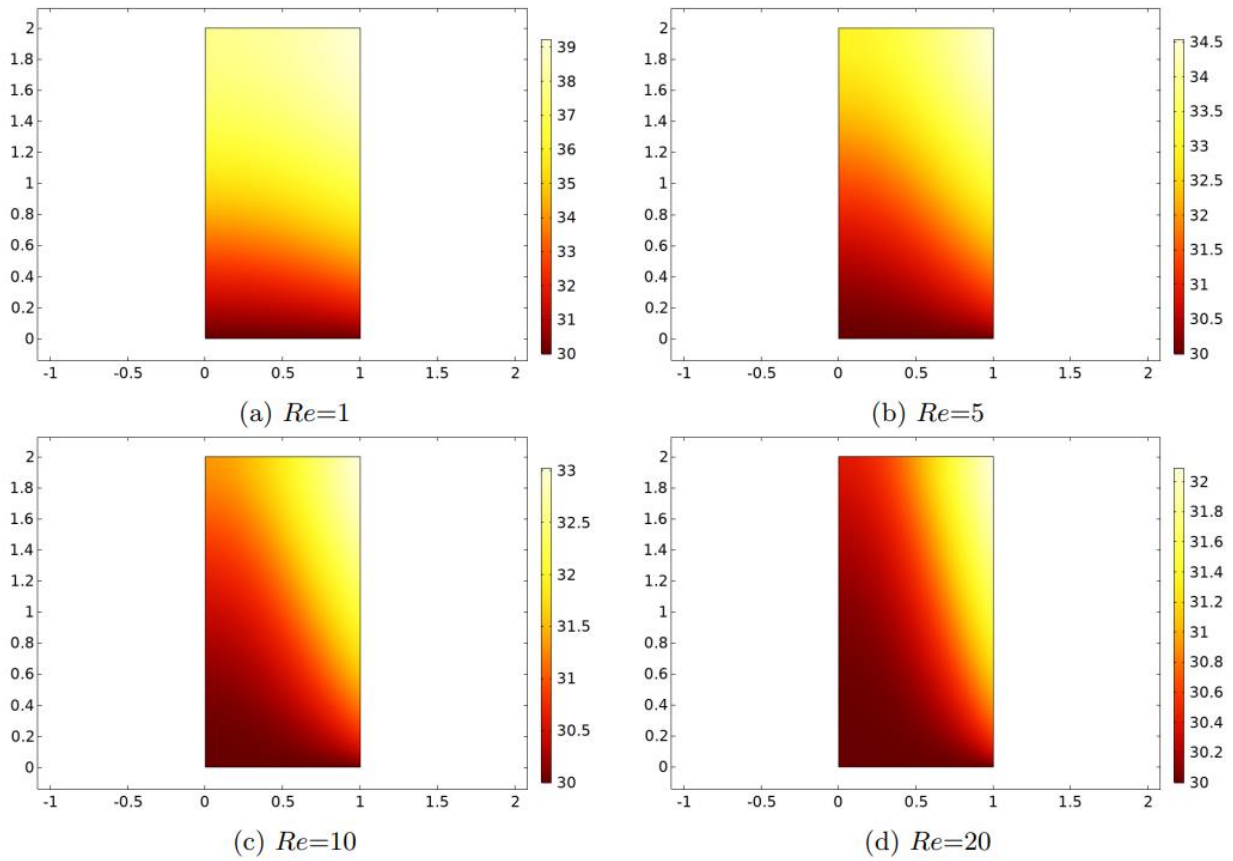


Figure 5: Effect Re on 2D Temperature field.

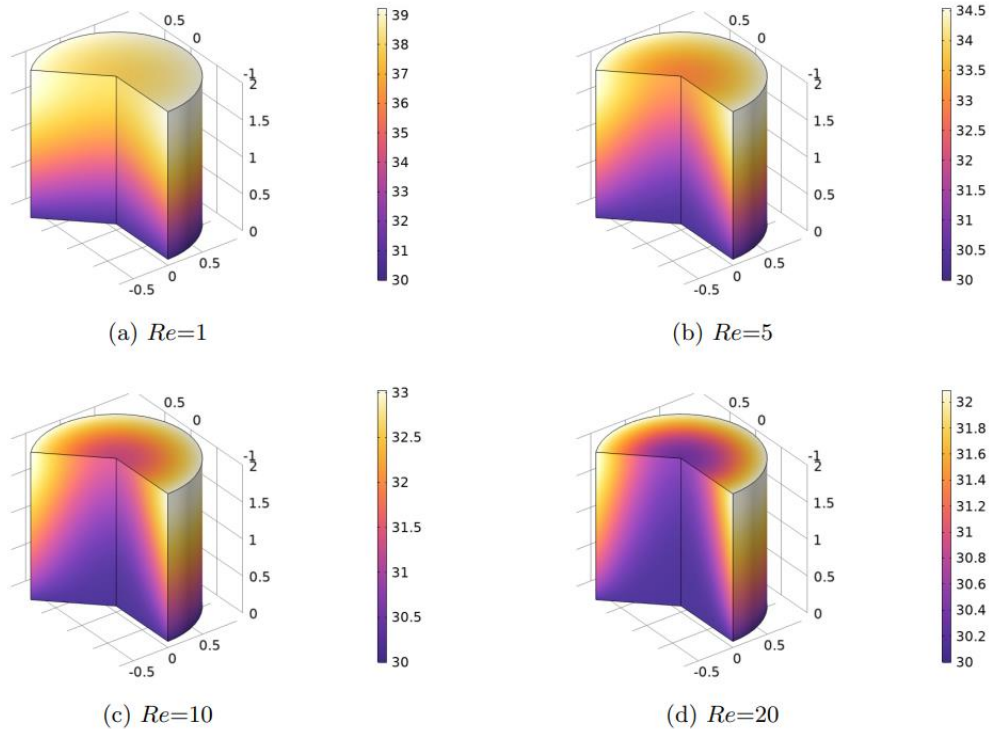


Figure 6: Effect Re on 3D Temperature field.



This article is licensed under the terms and conditions of the Creative Commons Attribution-NonCommercial 4.0 International (CC BY-NC 4.0) license.

NonCommercial 4.0 International (CC BY-NC 4.0 license)

(<http://creativecommons.org/licenses/by-nc/4.0/>).

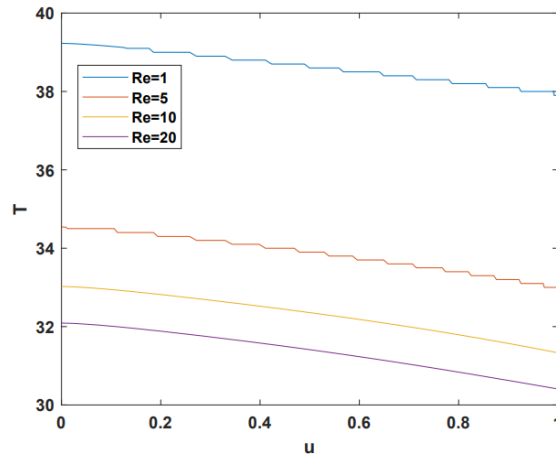


Figure 7: Relation between velocity and temperature with different (Re).

Pr-Variation: Similar to the Reynolds number, the Prandtl number is a significant factor in determining the change in axial temperature (T). Figures 8 and 9 show the influence of the Prandtl number on the temperature distribution in 2D and 3D with constant viscosity and Reynolds number ($Re = \mu = 1$). As the Prandtl number increases, the thermal boundary layer thickness decreases, leading to a corresponding decrease in the temperature distribution and the results are consistent with the findings of [24]. For velocity and pressure, Figure 10 shows that, changing the Prandtl number has no direct effect on the axial velocity and pressure.

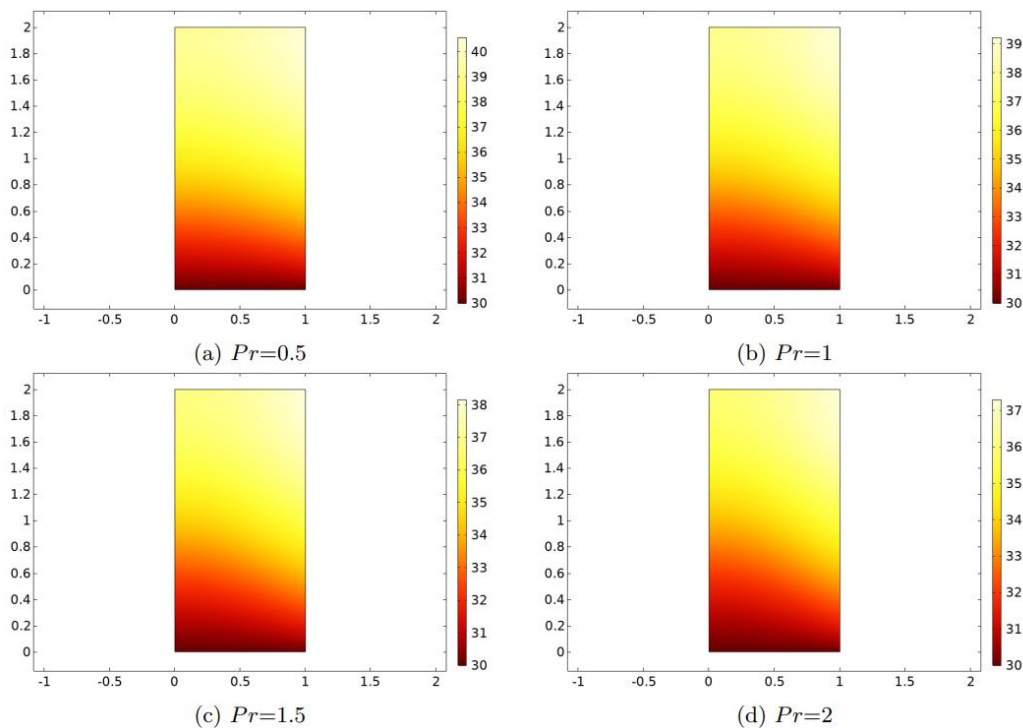


Figure 8: Influence Pr on 2D Temperature field.



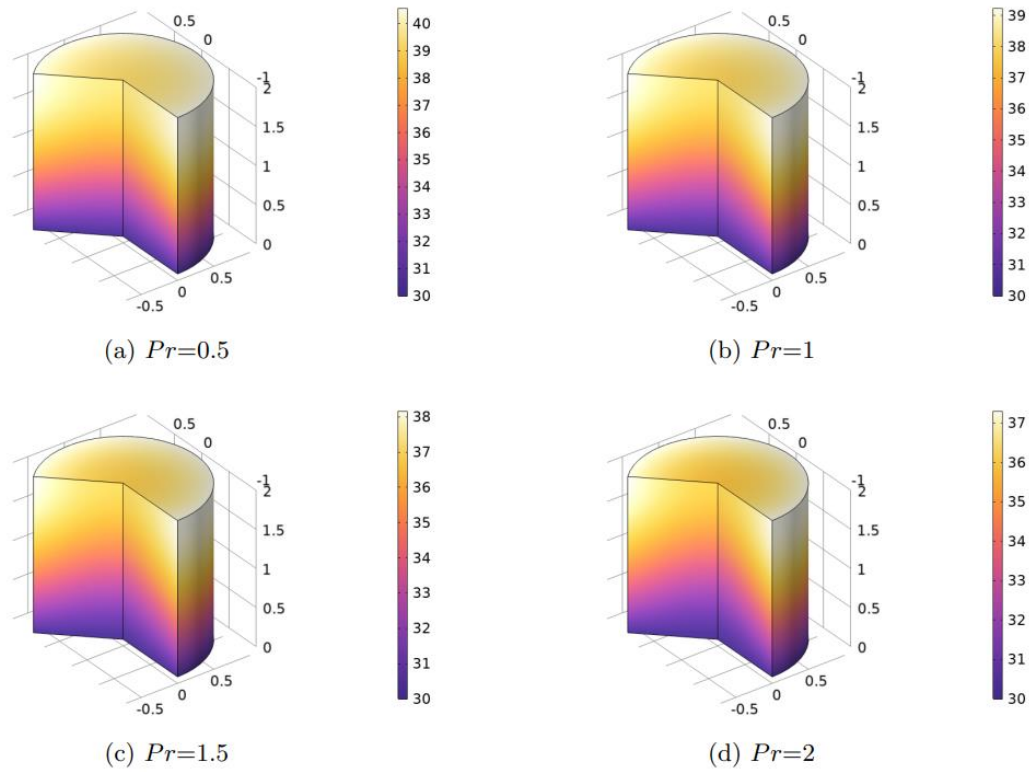


Figure 9: Influence of Pr on 3D Temperature field.

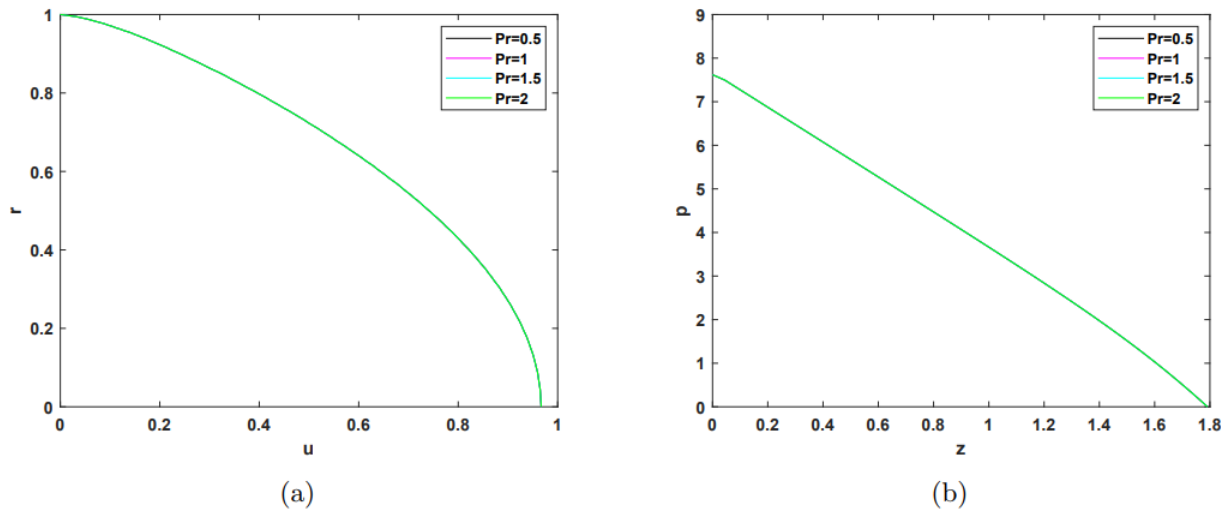


Figure 10: Effect Pr on (a)Velocity and (b)Pressure.

Convergence of proposed method: At the end, the convergence of axial velocity, pressure and temperature that had been evaluated by using the new algorithm (DTG/PC) is illustrated in Figure 11, as it is clear that convergence is excellent and effective.

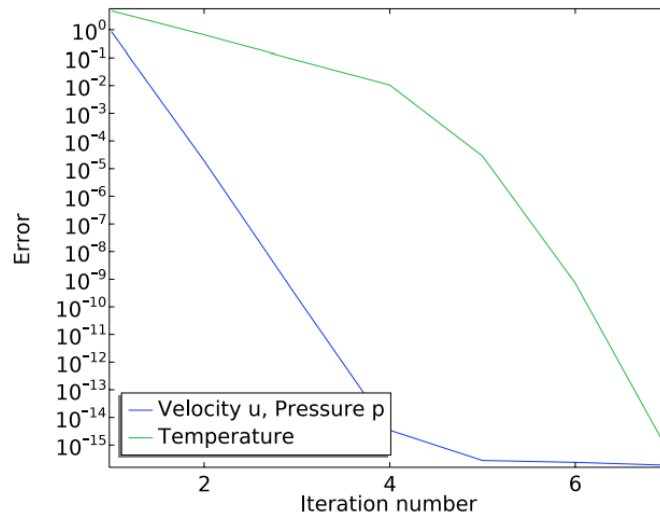


Figure 11: Rate of Convergence.

6. Conclusion

This study focuses on the derivation of the energy equation in cylindrical coordinates, followed by numerical simulations of laminar incompressible Newtonian fluid under thermal conditions using the newly developed Taylor-Galerkin/pressure-correction method in a cylindrical coordinate system. The developed numerical method demonstrated high accuracy and efficiency in obtaining results. The impact of the Reynolds number (Re) on the velocity, pressure, and temperature of the fluid was reported. The results revealed a direct relationship of (Re) with velocity and pressure and an inverse relationship with temperature. Additionally, the results clarified the direct inverse relationship between fluid velocity and temperature, where an increase in fluid velocity led to a decrease in heat accessibility. The effect of the Prandtl number (Pr) on temperature was also tested, and it was found that there was a strong effect, including an increase in fluid temperature with a decrease in (Pr). All of these tests produced very good results and were consistent with the expected physical behavior.



References

- [1] R. W. Lewis, P. Nithiarasu, K. N. Seetharamu, Fundamentals of the finite element method for heat and fluid flow. John Wiley & Sons, 2004. <https://doi.org/10.1002/0470014164>
- [2] M. K. Khandelwal, N. Singh, Stability of non-isothermal annular Poiseuille flow with viscosity stratification. International Communications in Heat and Mass Transfer 138 (2022): 106359. <https://doi.org/10.1016/j.icheatmasstransfer.2022.106359>
- [3] A. A. Cuadri R. Gallego, M.J. Martín-Alfonso, C. Delgado-Sánchez, E. Cortés-Triviño, A. Tenorio-Alfonso, A.M. Borrero-López, F.J. Ortega, A Mathcad-based educational experience to address the design of nonisothermal plug flow reactors, Comp Applications Eng Edu., 30 (2022)1145-1160. <https://doi.org/10.1002/cae.22509>
- [4] D.M. Hawken, H.R. Tamaddon-Jahromi, P. Townsend, M. F. Webster Taylor–Galerkin-based algorithm for viscous incompressible flow, Int. J Numer Meth Fluids 10(1990)327-351. <https://doi.org/10.1002/flid.1650100307>
- [5] V. Ngamaramvaranggul, M.F. Webster, Computation of Free Surface Flows with a Taylor-Galerkin/Pressure-correction Algorithm, Int. J. Num. Meth. Fluids, 27(1999), <https://doi.org/10.1016/j.cam.2016.06.007>
- [6] V. Ngamaramvaranggul, and N. Thongjub, Simulation of Die-swell Flow for Wet Powder Mass Extrusion in Pharmaceutical Process, Appl. Sci. Eng. Prog., 13 (2020)354-361. <https://doi.org/10.14416/j.asep.2020.03.004>
- [7] A. Al-Haboobi, G. A. Al-Juaifri, and A. H. Al-Muslimawi, Numerical study of Newtonian laminar Flow around circular and square cylinders. Results in Control and Optimization 14 (2024)100328. <https://doi.org/10.1016/j.rico.2023.100328>
- [8] A.H. Al-Muslimawi, Theoretical and numerical studies of die swell flow, Korea-Australia Rheology J, 28 (2016) 229-236, <https://doi.org/10.1007/s13367-016-0023-6>
- [9] H. Abro, A. Baloch, Â.H. Kazi, Â.M. Ali Nizamani, Quasi 3D finite element algorithm for rotating mixing flows. Mehran University Res J Eng. Technolo, 38(2019)479-486, <https://doi.org/10.22581/muet1982.1902.22>
- [10] A. J. Chorin, Numerical solution of the Navier-Stokes equations. Mathematics of computation 22.104 (1968): 745-762. <https://doi.org/10.1090/S0025-5718-1968-0242392-2>
- [11] P. M. Gresho, et al. Time-dependent FEM solution of the incompressible Navier--Stokes equations in two-and three-dimensions. No. UCRL--81323. California Univ., 1978.



- [12] J. Donea, S. Giuliani, H. Laval, L. Quartapelle, Finite element solution of the unsteady Navier-Stokes equations by a fractional step method. *Computer Methods in Applied Mechanics and Engineering* 30 (1982)53-73. [https://doi.org/10.1016/0045-7825\(82\)90054-8](https://doi.org/10.1016/0045-7825(82)90054-8)
- [13] M. Kawahara, K. Ohmiya, Finite element analysis of density flow using the velocity correction method. *International Journal for numerical methods in Fluids* 5.11 (1985)981-993. <https://doi.org/10.1002/flid.1650051104>
- [14] A. Al-Haboobi, A. H. Al-Muslimawi, Novel algorithm for compressible Newtonian axisymmetric thermal flow. *International Journal of Modern Physics C* 2450025 (2024): 17. <https://doi.org/10.1142/S0129183124500256>
- [15] F. Ali, M. Zahid, Y. Hou, J. Manafian, M.A. Rana, A. Hajar, A theoretical study of reverse roll coating for a non-isothermal third-grade fluid under lubrication approximation theory. *Mathematical Problems in Engineering* 2022 (2022). <https://doi.org/10.1155/2022/5029132>
- [16] A. H. Ganie, A.H. Ganie, A.A. Memon, M.A Memon, A.M. Al-Bugami, K. Bhatti, I. Khan, Numerical analysis of laminar flow and heat transfer through a rectangular channel containing perforated plate at different angles. *Energy Reports* 8 (2022): 539-550. <https://doi.org/10.1016/j.egy.2021.11.232>
- [17] F. P. Incropera, et al, *Fundamentals of heat and mass transfer*. Vol. 6. New York: Wiley, 1996.
- [18] J. D. Hoffman, *Numerical Methods for Engineers and Scientists*, Second Edition Revised and Expanded, by Marcel Dekker. Inc. New York 2001.
- [19] K. A. Hoffmann, S. T. Chiang, *Computational fluid dynamics volume I*. Engineering education system 2000.
- [20] T. Heuzé, Lax-Wendroff schemes for elastic-plastic solids. *Journal of Computational Physics* 396 (2019): 89-105. <https://doi.org/10.1016/j.jcp.2019.06.050>
- [21] P. K. Kundu, I. M. Cohen, D. R. Dowling, *Fluid mechanics*. Academic press, 2015, doi.org/10.1115/1.1424298
- [22] R. B. Bird, Transport phenomena. *Appl. Mech. Rev.* 55.1 2002: R1-R4. <https://doi.org/10.1115/1.1424298>



- [23] J. L. Plawsky, Transport phenomena fundamentals. CRC press, 2020, doi.org/10.1201/9781315113388
- [24] S. Mukhopadhyay, K. Bhattacharyya, T. Hayat, Exact solutions for the flow of Casson fluid over a stretching surface with transpiration and heat transfer effects. Chinese Physics B 22.11 (2013): 114701. <https://doi.org/10.1088/1674-1056/22/11/114701>

خوارزمية جديدة لحل التدفق الحراري النيوتوني في قناة مستقيمة محورية

انس الحبوبي – علاء حسن المسلماوي

جامعة البصرة، كلية العلوم، قسم الرياضيات

المستخلص

في هذه الدراسة ، تمت مناقشة ثلاث قضايا رئيسية في تدفق السوائل. أولاً ، يتم اشتقاق معادلة الطاقة ضمن إحدائيات أسطوانية ، وهو ما لم يتناوله الباحثون من قبل. ثانياً ، قمنا بتطوير خوارزمية جديدة لحل المعادلات الحاكمة التي تصف التدفقات النيوتونية غير القابلة للضغط تحت الظروف الحرارية. تم إنشاء هذه الخوارزمية بناءً على ما يسمى طريقة العنصر المحدود Taylor-Galerkin / Pressure-Correction بمساعدة مخطط Lax-Wendroff المكون من خطوتين. أخيراً ، قمنا بدراسة تأثير الأرقام غير الأبعاد ، مثل رقم رينولدز (Re) ورقم Prandtl (Pr) ، على السرعة والضغط ودرجة الحرارة. أظهرت النتائج أن الطريقة المطورة تتوافق مع الظواهر الفيزيائية الراسخة ودراسات أخرى.

